

# Thermodynamics of Yeast Cell Osmoregulation: Passive Mechanisms

P. GERVAIS \*, P. MOLIN, P. A. MARECHAL and C. HERAIL-FOUSSEREAU  
*Laboratoire Génie des Procédés Alimentaires et Biotechnologiques, ENSBANA – Université de Bourgogne, 1 Esplanade Erasme, F-21000 Dijon, France. Tel. 33 80 39 66 54; Fax 33 80 39 66 11; e-mail: gervais@u-bourgogne.fr (\*author for correspondence)*

(Received: 28 December 1995; accepted in final form: 1 March 1996)

**Abstract.** The response of yeast cells to osmotic pressure variations of the medium were studied through the kinetics of cell-volume modifications corresponding to the mass transfer of water and solutes. Osmotic variations were made by modification of the concentration of an external binary solution (polyol/water) without nutritive components. Two phases were distinguished in the thermodynamic response. A transient phase following an osmotic shift, which is characterised by rapid water transfer across the cell membrane and whose kinetics determine cell viability; then, a steady-state phase is reached when the cell volume becomes quasi-constant. The response of the cell during the transient phase depends on the level of the osmotic stress, and hence of the osmotic pressure of the medium. In the range of weak osmotic pressures, the metabolism of the cell is preserved through the maintenance of the intracellular turgor pressure. On the other hand in the range of high osmotic pressures of the medium, yeast cells behave as osmometers and no further metabolism occurs.

**Key words:** Cell volume, Osmotic pressure, Osmotic stress, Yeasts

## 1. Introduction

Under particular conditions, cells behave as osmometers when subjected to osmotic stress, but for most of the time, passive diffusion of external solutes and the biological response occur simultaneously [19]. Nevertheless, the time constant of the thermodynamic response linked to the transfer of water is obviously shorter [12, 17] than the time constant observed for biological responses [23]. Workers have used thermodynamics in order to quantify the cell-volume response [13] and to identify certain cell parameters such as  $L_p$  (hydraulic permeability),  $\varepsilon$  (cell-wall volumetric elastic modulus),  $b$  (non-osmotic volume), in numerous areas and particularly for the cryopreservation of animal cells [20]. In the case of walled cells such as yeast, the turgor pressure ( $\Delta P$ ) which is equilibrated by the wall resistance is an important parameter of cell osmoregulation. The normal turgor pressure of *Saccharomyces cerevisiae* has been estimated between  $-0.5$  and  $-1.5$  MPa by previous authors [3, 10, 14]. Whilst an important theoretical review was made by Nobel [18], it is important to clarify some kinetic aspects of the thermodynamic response to osmotic stress, which are not always taken into account.

In this work only the passive thermodynamic response will be studied through the use of non-nutritive solutes as osmotic agents.

When a cell is subjected to osmotic stress with a binary solution (water-solute), such as a step-wise increase of fixed intensity, two thermodynamics phases must be considered:

- *A Transient phase* which corresponds to the thermodynamic response of the cell versus time and so to the mechanisms of water transfer through the cell membrane. In previous work [2], this transient phase has been characterised by its very short time constant (less than 1 sec). During this time the cell can be injured by the water flow from the cell to the medium which can damage the membrane. Indeed this cell-water flow rate is directly proportional to the water potential gradient between the intra- and extra-cellular media and is only limited by the hydraulic permeability ( $L_p$ ) of the membrane.
- *A steady-state phase*. The previous transient phase allows the cell to reach a steady-state phase characterized by a constant volume. The final volume depends on the stress intensity as proposed by numerous author [4, 16, 18, 19].

In the literature many workers have studied the steady-state phase with the use of the Boyle–Van't Hoff equation which can be written:

$$\Pi(V - b) = (\Sigma\Phi_s n_s)RT = nRT, \quad (1)$$

with  $\Pi$ : osmotic pressure of the medium ( $Pa$ );  $V$ : cell volume ( $m^3$ );  $b$ : non-osmotic volume ( $m^3$ );  $n = \Sigma\Phi_s n_s$ : apparent number of osmotically active moles;  $n_s$ : number of solutes molecules;  $\Phi_s$ : osmotic coefficient;  $R$ : constant of ideal gas ( $J \cdot mol^{-1} \cdot K^{-1}$ );  $T$ : temperature (K). From this equation it can be deduced that when the steady state is reached, the volume will be inversely proportional to the osmotic pressure:

$$V - b = \frac{nRT}{\Pi}. \quad (2)$$

There are numerous data presented which attempt to link two variables ( $V, 1/\Pi$ ) and which show experimental curves following the model given in Figure 1 [15–17]. Such a curve is representative of the steady-state volume of a cell subjected to different osmotic pressures. This curve allows the graphic determination of three points: A = beginning of the plasmolysis; B = maximum experimental values of osmotic pressure; C = non-osmotic volume.

There is general agreement in the literature and the curve can be divided into two linear parts. The first horizontal part corresponds to the osmotic range from  $\Pi_0$  to  $\Pi_A$ , i.e. from point O to A (see Fig. 1) the cell subjected to an osmotic step, maintains its initial volume after a residence time of a few minutes in the binary solution. It could be postulated that the steady-state values of osmotic pressure of this range were always superior to the internal turgor pressure of the cell which is

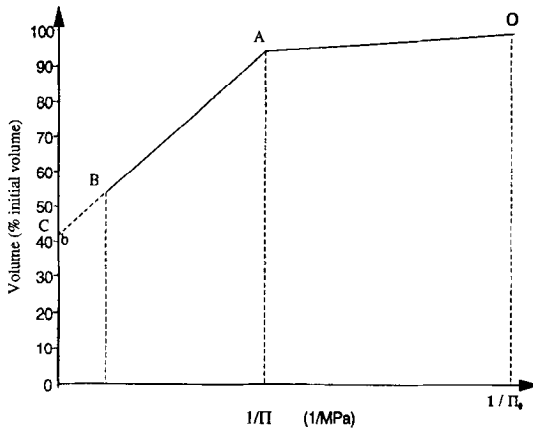


Figure 1. Shape of cell relative volume evolution as a function of  $1/\Pi$  (MPa), where  $\Pi$  is the external osmotic pressure.  $\Pi_0$  is the initial osmotic pressure of the medium.

initially equilibrated by the cell-wall rigidity. So, the increase of external osmotic pressure was balanced by an increase of turgor pressure ( $\Delta P$ ) and a necessitating modification of the cell-membrane elasticity. Point A corresponds to a  $\Delta P = 0$  and initial values of  $\Delta P$  varied depending on the species from 2 KPa for animal cells to 3 MPa for osmotolerant fungi [8]. For *Saccharomyces cerevisiae* the values of  $\Delta P$  obtained by previous workers varied from the range 0.3 MPa/1 MPa [3] to 1.33 MPa [10] and 2.9 MPa [1]. From  $\Pi_A$  to greater values the turgor pressure must be almost 0 and the experimental curves found in the literature (until point B) were following the Boyle–Van't Hoff relation: an increase in osmotic pressure corresponds to a decrease in cell volume.

The extrapolation from point B to C (where external osmotic pressure is infinite) allows the determination of the non-osmotic volume,  $b$ , which corresponds to point C on the curve (Fig. 1). This scheme which was used by numerous workers (10, 16, 19) requires further discussion.

The yeast-cell osmoregulation mechanism will be examined in this work for two successive ranges of osmotic pressure increases:

- In the range between  $\Pi_0$  and  $\Pi_A$ , i.e. when the initial osmotic pressure is between  $\Pi_0$  and  $\Pi_A$  and if the osmotic shift does not exceed the  $\Pi_A$  value.
- In the range above  $\Pi_A$ , i.e. when the osmotic shift exceeds the  $\Pi_A$  value.

For each range studied the cell-volume response to hyperosmotic stress is analysed in this work through two successive phases: the steady-state phase which corresponds to the steady-state volume reached by the cell after stress and the transient phase which corresponds to the volume evolution during stress.

## 2. Material and Methods

All results concerning cell-volume measurement which are presented in this paper have been obtained through the use of a visualization chamber coupled to a microscopic design and an Image Analysis System which has been described in a previous paper [2]. The microorganism used was *Saccharomyces cerevisiae* CBS 1171 and the cultivation conditions and the viability measurements correspond exactly to those related in previous work [7]. Osmotic perturbations were realized through the use of high concentrated binary (water/polyol) solutions and in all cases the initial osmotic pressure of the nutritive medium was fixed at 1.36 MPa through glycerol addition. Osmotic pressure levels of different liquid media were verified through the use of a dew point osmometer (DECAGON CX100, U.S.A.).

## 3. Results and Discussion

As previously discussed, two cell compartments were distinguished: the case of application of osmotic shifts inferior to the initial cell turgor pressure and corresponding to an overpressured cell situation; and the case of application of osmotic shifts greater than this turgor value, and then, corresponding to a cell situation of perfect osmometer.

### 3.1. THE OVERPRESSURED CELL SITUATION

#### 3.1.1. Study of the steady-state phase

Previous results presented in Figure 2 for *Saccharomyces cerevisiae* [11] confirm the previous theoretical curve (Fig. 1) and show that the stationary volume was relatively constant from initial pressure to the pressure at point A. During this phase a thermodynamic equilibrium can be written as follows, since the water chemical potentials of the intra- and extra-cellular media are equal [8, 22]:

$$\mu_{w_0} - \mu_{w_i} = \bar{V}_w(\Pi_i - \Pi_0 + P_0 - P_i + \tau_i - \tau_0) = 0 \quad (3)$$

with

$$\Pi = -\frac{RT \ln a_w}{\bar{V}_w}, \quad (4)$$

where  $a_w$ : water activity (dimensionless);  $\Pi$ : osmotic pressure (Pa);  $\Pi_0$ : external osmotic pressure (Pa);  $\Pi_i$ : cell osmotic pressure (Pa);  $\bar{V}_w$ : water molar partial volume ( $\text{m}^3$ );  $\tau$ : suction pressure or matrix potential (Pa);  $P_i$ : internal hydrostatic pressure (Pa);  $P_0$ : external hydrostatic pressure (Pa);  $(P_i - P_0) = \Delta P$ : turgor pressure (Pa);  $\mu_{w_0}$ : external chemical potential of water ( $J \cdot \text{mol}^{-1}$ );  $\mu_{w_i}$ : chemical water potential of the cell ( $J \cdot \text{mol}^{-1}$ ).

A first hypothesis allows simplification of Equation 3; even if the internal cell medium was not only composed by a solution, all interactions between water and

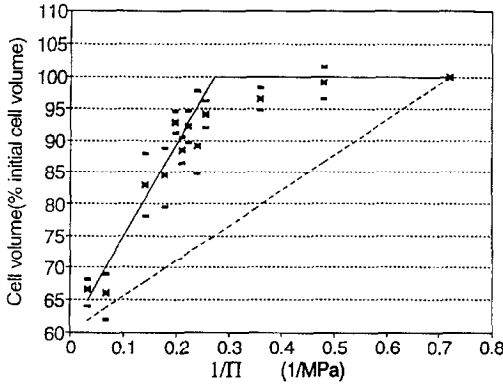


Figure 2. Evolution of the relative volume of *Saccharomyces cerevisiae* as a function of  $1/\Pi$  (MPa), where  $\Pi$  is the external osmotic pressure. Depressor used:  $\times$ , glycerol experimental data, with confidence interval at 95 %; ---, expected answer according to Boyle–Van't Hoff law without taking the turgor pressure into account; —, expected answer according to Boyle–Van't Hoff law, with taking the turgor pressure into account.

solid macromolecules can be neglected and so the matrix potential relative to these macromolecular interactions is not taken into account. Therefore,  $\tau_i = \tau_0 = 0$ .

So the thermodynamic steady-state phase of a cell placed in a liquid medium at an osmotic pressure of  $\Pi_0$  ( $\Pi_0 < \Pi_A$ ) could be represented by the following equation:

$$\Pi_i - \Pi_0 = P_i - P_0 = \Delta P. \quad (5)$$

This very simple equation allows to understand how the osmotic potential gradient between intra- and extra-cellular media involves an hydrostatic pressure gradient which is equilibrated by the cell membrane turgor.

### 3.1.2. Study of the transient phase: kinetics of cell-volume variation

Cultivations of *Saccharomyces cerevisiae* of two different physiological stages (48 h, 96 h) were submitted to successive osmotic step changes of the external medium. The mean cell-volume variations of these cells corresponding to each shift application are given in Figure 3. For both cell stages the cell volume was found to remain constant when the osmotic step change was inferior to 0.18 MPa (corresponding to an initial cell turgor pressure value of  $\Delta P = 0.18$  MPa).

So, when the external osmotic pressure value increases from  $\Pi_0^1$  to  $\Pi_0^2$  with  $\Pi_0^2 < \Pi_A$  (see Fig. 1) due to a sudden osmotic step increase, no or very few volume variations were observed. So, in this case the transient phase did not concern the cell volume but other cell parameters and particularly the turgor pressure  $\Delta P$  and the cell-volume elasticity modulus ( $\varepsilon$ ). Indeed, the theoretical thermodynamic response of the cell would have provoked a large and fast exit of water from the cell (as predicted by the Boyle–Van't Hoff law) and so a great decrease in cell volume.

Table I. Evolution of cell and media parameters after an application of an osmotic shift inferior to the turgor pressure

	External pressure	Internal pressure	Cell volume	Turgor Pressure
Stage 1 (initial)	$\Pi_0^1$	$\Pi_i^1$	$V_1$	$\Delta P_1$
Stage 2	$\Pi_0^2$	$\Pi_i^2$	$V_2$	$\Delta P_2$

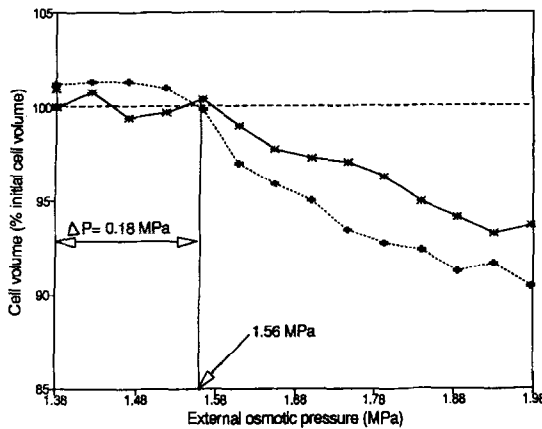


Figure 3. Relative cell volume versus external osmotic pressure. Cells have been submitted to successive osmotic step changes of the external medium. Initially cells proceed from different physiological stages: - - - + - - - 48 h; — \* — 96 h.

In fact only very little water was flowing through the membrane due to the decrease of the turgor pressure between stage 1 ( $\Pi_0^1$ ) and stage 2 ( $\Pi_0^2$ ) as summarised in Table I.

Indeed, the volume observed is the same (see Fig. 3) for the two stages ( $V_2 \approx V_1$ ), so from the Boyle–Van't Hoff law,  $\Pi_i^2$  is very close to  $\Pi_i^1$ .

From Equation 5 it could be written:

$$\Pi_i^1 = \Pi_0^1 + \Delta P_1 \quad (6)$$

and

$$\Pi_i^2 = \Pi_0^2 + \Delta P_2. \quad (7)$$

As  $\Pi_0^2$  is greater than  $\Pi_0^1$ , and from Equations 6 and 7,  $\Delta P_2$  is obviously smaller than  $\Delta P_1$ . So stage 1 and stage 2 correspond to almost equivalent cell volumes but to different turgor pressure values. The difference of turgor pressure between

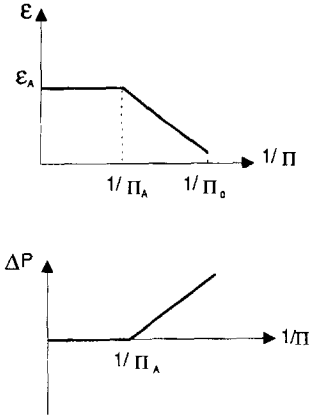


Figure 4. Proposed evolution of cell volumetric elasticity modulus ( $\epsilon$ ) and of the cell turgor pressure ( $\Delta P$ ) during the overpressured range.

these two stages, if the cell-wall volumetric elastic modulus ( $\epsilon$ , in Pa) is considered constant, would involve a cell-volume decrease equal to:

$$V_1 - V_2 = \frac{V_1(\Delta P_1 - \Delta P_2)}{\epsilon}. \quad (8)$$

As  $V_1 - V_2 \approx 0$  and  $\Delta P_2$  was smaller than  $\Delta P_1$ , then the wall-volumetric elastic modulus must have varied between stage 1 and stage 2. When the external osmotic pressure increases until  $\Pi_A$  then the  $\Delta P$  is almost equal to 0 and the cell-volume variation for greater osmotic pressure variation will follow the Boyle–Van't Hoff law. So in the overpressured range from  $\Pi_0$  to  $\Pi_A$ , for an osmotic increase of an intensity inferior to  $\Pi_A$ , there is no significant cell-volume variation of the yeast and it could be postulated that  $\Delta P$  was decreasing near to 0 and  $\epsilon$  was increasing to a constant value  $\epsilon_A$  as proposed (for a postulated linear relation) in Figure 4.

### 3.2. THE CELL 'OSMOMETER' SITUATION

As in the previous case, the effect of an osmotic perturbation on the cell volume is analysed for both steady-state and transient phases. In this case the osmotic perturbation intensity is greater than the  $\Pi_A$  value (see Fig. 1).

#### 3.2.1. Study of the steady-state phase

From the  $\Pi_A$  value and above, and because  $\Delta P = 0$ , the experimental curve up to point B could be fitted through the utilisation of the Boyle–Van't Hoff Law.

The initial equation is Equation 5 with  $\Delta P = 0$ , and  $\Pi_0 = \Pi_i$  which is, from Equation 4, equivalent to:

$$\Pi_0 = -\frac{RT \ln a_{w_i}}{\bar{V}_w} \quad (9)$$

The Boyle–Van't Hoff's law can be deduced from this equation as follows: using the hypothesis of ideal solutions, i.e. that the solutions remain sufficiently dilute to be considered as ideal and that the osmotic pressures are not too high ( $n_s \ll n_w$ ), it can be written as:

$$a_{w_i} = N_w = \frac{n_w}{n_w + n_s} = 1 - \frac{n_s}{n_w + n_s} \approx 1 - \frac{n_s}{n_w} \quad (10)$$

with  $N_w$ : water molar fraction;  $n_w$ : number of water molecules;  $n_s$ : number of solute molecules.

So

$$\ln a_{w_i} = \left(1 - \frac{n_s}{n_w}\right) \approx -\frac{n_s}{n_w}, \quad (11)$$

and by replacing  $\ln a_{w_i}$  by  $(-n_s/n_w)$ , Equation 9 becomes:

$$\Pi_0 = \frac{RTn_s}{n_w \bar{V}_w}, \quad (12)$$

$n_w \bar{V}_w$  is equal to the cell osmotic volume:  $(V - b)$ , so Equation 12 can be written:

$$\Pi_0(V - b) = RTn_s, \quad (13)$$

which is the classical expression for the Boyle–Van't Hoff law proposed in Equation 1.

Equation 13 must be used very carefully when applied to the whole range of osmotic pressure variations. In fact, if the cell turgor pressure is not taken into account, important errors could be made between estimated and observed values as proposed in Figure 2. For real solutions, but only in the case of diluted and non-electrolytic solutions, previous equations lead to:

$$\Pi = RT \frac{\sum \gamma_s n_s^i}{\bar{V}_w n_w^i}, \quad (14)$$

where  $\gamma_s$  is the activity coefficient (dimensionless) for solute  $S$ ;  $n_s^i$  and  $n_w^i$  are the initial numbers of solutes and water molecules (respectively). With  $\bar{V}_w n_w^i = V - b$ , Equation 14 becomes:

$$(\Pi_0)(V - b) = RT(\sum \gamma_s n_s^i). \quad (15)$$

This equation is representative of the cell thermodynamic steady state in the considered range of osmotic pressure (i.e. greater than  $\Pi_A$ ).

The restrictive application of these law to diluted solutions could be discussed as follows: Since the Boyle–Van't Hoff's Law, which is equivalent to Equation 15,



was derived from thermodynamic laws but only for dilute solutions, the linear part of the steady-state curve (from point A to point B) is only theoretically justified, if the solution can be considered to be diluted.

For instance, if it is accepted that the ratio  $n_s/(n_s + n_w)$  is equal to  $n_s/n_w$  with a relative error of 10%, then:

$$\left( \frac{n_s}{n_w} \leq \frac{n_s}{n_s + n_w} + 0.1 \frac{n_s}{n_s + n_w} \right),$$

and  $n_w$  must be equal to or greater than  $10 n_s$ , which approximately corresponds to a solution with a water activity limit value of 0.91 or osmotic pressure value of about 13 MPa (this value is weakly dependent on  $V_w$  and  $T$  variations, see Equation 4).

So the extrapolation of this curve to point C, which corresponds to the non-osmotic volume and an infinite osmotic pressure will involve an important error, and therefore the majority of previous calculated non osmotic volumes ( $b$ ) have been underestimated.

### 3.2.2. Study of the transient phase: kinetics of cell-volume variation

The steady-state equilibrium of a cell corresponds to the asymptotic value of the volume kinetics when the cell is subjected to an osmotic stress.

The analysis of the Boyle–Van't Hoff's curve (Fig. 1) which corresponds to the stationary phase of the cell volume is required in order to understand the transient phase.

When the cell is subjected to an osmotic shift which corresponds to a final value of  $\Pi_2 (\Pi_2 > \Pi_A)$ , the resulting transient curve is given by Figure 5 for two different solutes [11]. The kinetic evolution ( $V = f(t)$ ) corresponds to the transient phase and depends on the nature of the osmotic entry: step-wise increase or linear increase, and on the nature of the solute used: a permeant one such as glycerol [4, 5] or a non-permeant one such as sorbitol [17] as shown in Figure 5.

## 3.3. CELL-VOLUME RESPONSE TO AN OSMOTIC STEP INCREASE OF THE EXTERNAL MEDIUM

### 3.3.1. Case of a non-permeant solute depressor

In case of the use of sorbitol, which is a non-permeant solute, the application of irreversible thermodynamic laws proposed by Kedem and Katchalsky [9] allows the net volume water flow rate ( $J_w$ ) between intra- and extra-cellular medium to be written as:

$$J_w = -\frac{1}{A} \frac{dV}{dt} = L_p(\Delta P - \sigma \Delta \Pi), \quad (16)$$

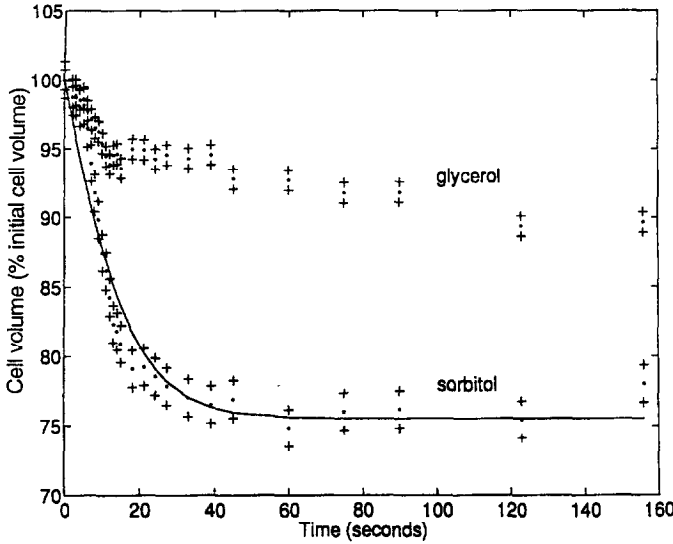


Figure 5. Relative volume evolution of *Saccharomyces cerevisiae* versus time, after an osmotic step of 1.38 MPa realized with glycerol or with sorbitol. Confidence interval at 95 %. Narrow line: Predicted volume evolution by the Boyle-Van't Hoff law.

where  $A$ : surface of the cell ( $\text{m}^2$ );  $\sigma$ : reflection coefficient of the membrane;  $\Delta P$ : turgor pressure (Pa);  $V$ : volume of the cell ( $\text{m}^3$ );  $\Delta\Pi = (\Pi_i - \Pi_0)$ : gradient of osmotic pressure (Pa) between intra- and extra-cellular media.

This flow rate is experimentally similar to a flow rate induced by a hydrostatic pressure difference and is much greater (about  $10^3$ -fold [13]) than just a ficcan flow rate.

If it is considered that  $\Delta P$  tends to 0 during the transient phase and that the surface  $A$  remains constant with respect to time, Equation 16 becomes:

$$J_w = -\frac{1}{A} \frac{dV}{dt} = L_p \sigma (\Pi_0 - \Pi_i). \quad (17)$$

We assume that the physicochemical properties of the membrane remain constant during this short transient period and so  $L_p \sigma$  is a constant value also named  $K$ , which represents the hydraulic characteristics of the membrane, so:

$$-\frac{1}{A} \frac{dV}{dt} = K (\Pi_0 - \Pi_i), \quad (18)$$

where,  $\Pi_0$  = external osmotic pressure;  $\Pi_i$  = internal osmotic pressure at time  $t$ .

At each time  $t$  during the osmotic shift, with the assumption that only passive thermodynamic phenomena occur, the internal osmotic pressure  $\Pi_i$  can be related to the cell volume by the Boyle-Van't Hoff law as follows:

$$\Pi_i = \frac{RTn_s}{(V - b)}. \quad (19)$$

By replacing  $\Pi_i$  by this value, Equation 18 can be written:

$$-\frac{1}{A} \frac{dV}{dt} = K \left[ \Pi_0 - \frac{RTn_s}{V-b} \right]. \quad (20)$$

There is an analytical resolution of this differential equation which is:

$$\frac{1}{\Pi_0} (V - V_0) + \frac{V_f - b}{\Pi_0} \ln \left( \frac{V - V_f}{V_0 - V_f} \right) = -KAt, \quad (21)$$

with  $V_f = b + RTn_s/\Pi_0$ : final volume and  $K$ : adjustable variable ( $K = Lp \cdot \sigma$ ).

Such a model is compared in Figure 5 with experimental data obtained for *Saccharomyces cerevisiae* subjected to different intensities of osmotic step increases in water-sorbitol media. The model was found to fit very well with experimental data for coherent values of calculated parameters ( $V_f$  and  $Lp \cdot \sigma$ ) [11].

The curves showed that when the volume decreases, the rate of water flow also decreases. Indeed, the osmotic pressure gradient between the internal and external media normally decreased with the decrease in volume.

### 3.3.2. Case of a permeant solute depressor

Considering the permeant solute, glycerol. Whatever the range of stepwise increases in osmotic pressure, the curve fits well during the first 5 seconds as shown in Figure 5: then there is some discrepancy due to the glycerol diffusion into the intracellular medium. Indeed, glycerol flows inside, accompanied by water movement in order to restore the inverse osmotic pressure gradient. The diffusion rate of glycerol through the membrane was obviously less than the water diffusion rate and thermodynamic modelling was more complex in this case.

In the case of a high osmotic shift (of about 100 MPa) obtained through glycerol addition, *Saccharomyces cerevisiae* was found to reach a volume of  $0.40 V_0$  [12]. Such a volume must be compared to previous observed non-osmotic volume values for *Saccharomyces cerevisiae* of about  $0.4 V_0$  [6]. So the hypothesis that there is only a passive thermodynamic response in operation was confirmed, the osmotic pressure gradient is almost totally compensated by the volume variation.

### 3.4. CELL-VOLUME RESPONSE TO LINEAR INCREASES OF THE OSMOTIC PRESSURE OF THE EXTERNAL MEDIUM

In the case of a linear increase in osmotic pressure as proposed in a previous work [12], the evolution of the external osmotic pressure versus time ( $t$ ) is:  $\Pi_0 = K't$ . The previous differential equation (18) becomes:

$$-\frac{1}{A} \frac{dV}{dt} = K(\Pi_0 - \Pi_i) = K \left( K't - \frac{RTn_s}{V-b} \right). \quad (22)$$

Table II. Effect of rate of osmotic pressure increase on cell viability of *Saccharomyces cerevisiae* and on the initial water flow rate. Initial osmotic pressure, 1.38 MPa. Final osmotic pressure, 101 MPa. Depressor used: glycerol. Cultivation time: 48 h.

Rate of osmotic pressure increase (MPa/s)	Viability (% related to a control)	$\frac{dV}{dt}$ : Initial water flow rate related to initial volume (%/s)
Shock	20	29.5
0.055	46	0.108
0.0332	62	0.072
0.0237	80	0.036
0.0092	90	0.0318

Numerical resolution of this equation has been made and allows the fitting of experimental curves. The realization of linear increases of osmotic pressure was found to decrease the instantaneous water flow rate which allows the preservation of the membrane integrity. So for very high (but slow) increases in osmotic pressure, the final volume was found to be the same as the one that was obtained with an osmotic stepwise realization but the viability was conserved as shown in Table II. The faster the shift of osmotic pressure was realized the greater the decrease in viability was observed. This loss in viability could be explained by the high flow of water across the cell membrane [12].

Very great differences in viability could be observed and a high viability level for very high osmotic pressure values (101 MPa) has been found for the weakest slopes used.

#### 4. Conclusion

Stationary phase and transient phase, which have been analysed in terms of cell-volume variation, have also great effects on cell viability [7].

An explanation of such viability can be found from thermodynamics. The curves  $V = f(\Pi)$  for the different values of the slopes of linear increases in osmotic pressure shows that the rate of increase does not modify the final cell volume for an osmotic pressure value. On the contrary, the flow rate of water related to the surface unity of the membrane was greatly dependent on such a rate; so the mortality factor should be assumed to be the membrane injury and the exit of protoplasmic material due to an important water flow rate, as proposed previously by Steponkus [21] for cell injury by freezing.

In the case of the study of stationary phase which concerned only cells which have survived the osmotic pressure variation; the following conclusions could be made:

- For a weak increase of the external osmotic pressure (until point A of Fig. 1) the osmotic pressure level of the medium was compensated by the cell turgor pressure and so allowed the maintenance of the cell volume.
- For higher increases (from point A to B of Fig. 1) the turgor pressure was null, could not maintain the cell volume, and the cell behaved as an osmometer until the non-osmotic volume was reached.

This study focused only on the passive thermodynamical response of the cells and further work will study the biological response of the cells through the addition of nutrients in the hypertonic solutions.

## References

1. Arnold, W. N. and Lacy, J. S.: Permeability of the cell envelope and osmotic behavior in *Saccharomyces cerevisiae*, *J. Bacteriol.* **137** (1977), 564–571.
2. Berner, J. -L. and Gervais, P.: A new visualization chamber to study the transient volumetric response of yeast cells submitted to osmotic shifts, *Biotechnol. Bioeng.* **43** (1994), 165–170.
3. Brown, A. D.: *Microbial Water Stress Physiology, Principles and Perspectives*, Wiley, Chichester, England, 1990.
4. Dick, D. A. T.: *Cell Water*, Molecular Biology and Medicine Series, Bittar, Oxford University Press, 1966.
5. Edgley, M. and Brown, A. D.: Response of xerotolerant and non-tolerant yeasts to water stress, *J. Gen. Microbiol.* **104** (1978), 343–345.
6. Gelinias, P., Toupin C. J. and Goulet, J.: Cell water permeability and cryotolerance of *Saccharomyces cerevisiae*, *Lett. Appl. Microbiol.*, **12** (1991), 236–240.
7. Gervais, P., Marechal, P. -A., and Molin, P.: Effects of the kinetics of osmotic pressure variation on yeast viability, *Biotechnol. Bioeng.* **40** (1992), 1435–1439.
8. Griffin, D. M.: Water and microbial stress, *Adv. Microb. Ecol.* **5** (1981), 91–136.
9. Kedem, O. and Katchalsky, A.: Thermodynamic analysis of the permeability of biological membranes to non-electrolytes, *Biochim. Biophys. Acta*, **27** (1958), 229–246.
10. Levin, R. L.: Water permeability of yeast cells at sub-zero temperatures, *J. Membrane Biol.* **46** (1979), 91–124.
11. Marechal, P. A.: *Étude de la réponse cellulaire des levures soumises à des variations contrôlées du potentiel hydrique*, Ph.D. Thesis, Université de Bourgogne, France, 1992.
12. Marechal, P. A. and Gervais, P.: Yeast viability related to the water potential variation: influence of the transient phase, *Appl. Microbiol. Biotechnol.* **42** (1994), 617–622.
13. Mauro, A.: Nature of solvent transfer in osmosis, *Science*, **26** (1957), 252–253.
14. Meikle, A. J., Reed, R. H., and Gadd, G. M.: Osmotic adjustment and the accumulation of organic solutes in whole cells and protoplasts of *Saccharomyces cerevisiae*, *J. Gen. Microbiol.* **134** (1988), 3049–3060.
15. Morris, G. J., Winters, L., Coulson, G. E., and Clarke, K. J.: Effect of osmotic stress on the ultrastructure and viability of the yeast *Saccharomyces cerevisiae*, *J. Gen. Microbiol.* **129** (1983), 2023–2034.
16. Munns, R., Greenway, H., Setter, T. L., and Kuo, J.: Turgor pressure, volumetric elastic modulus, osmotic volume and ultrastructure of *Chlorella emersonii* grown at high and low external NaCl, *J. Exp. Bot.* **34** (1983), 144–145.
17. Niedermeyer, W., Parish, G. R., and Moor, H.: Reactions of yeast cells to glycerol treatment, *Protoplasma* **92** (1977), 177–193.
18. Nobel, P. S.: The Boyle–Van't Hoff relation, *J. Theor. Biol.* **23** (1969), 375–379.
19. Reed, R. H.: Transient breakdown in the selective permeability of the plasma membrane of *Chlorella emersonii* in response to hyperosmotic shock: Implication for cell water relations and osmotic adjustment, *J. Membrane Biol.* **82** (1984), 83–88.

20. Schwartz, G. J. and Diller, K. R.: Osmotic response of individual during freezing, *Cryobiology* **20** (1983), 61–77.
21. Steponkus, P.: Membrane destabilization resulting from freeze-induced dehydration, in *Cryo 87: 24th Annual Meeting*, Society for Cryobiology, Edmonton, Canada, 1987.
22. Toupin, C. J., Marcotte, M., and Le Maguer, M.: Osmotically-induced mass transfer in plant storage tissues: a mathematical model, Part 1, *J. Food Eng.* **10** (1989), 13–38.
23. Zimmermann, U.: Physics of turgor and osmoregulation, *Annu. Rev. Plant Phys.* **29** (1978), 121–148.